Layered Polyelectrolyte Films as Selective, Ultrathin Barriers for Anion Transport

Jeremy J. Harris, Jacqueline L. Stair, and Merlin L. Bruening*

Department of Chemistry, Michigan State University, East Lansing, Michigan 48824

Received February 7, 2000. Revised Manuscript Received April 24, 2000

Synthesis of high-flux composite membranes requires methods for deposition of ultrathin, defect-free films on highly permeable supports. Layer-by-layer deposition of polyelectrolytes on porous alumina (0.02 μm pore diameter) produces such membranes. Electron microscopy shows that five bilayers (<25 nm) of poly(allylamine hydrochloride) (PAH)/poly(styrenesulfonate) (PSS) are sufficient to cover porous alumina and that underlying pores are not clogged during the deposition process. The selectivity of anion transport through these membranes increases with the number of bilayers until the substrate is fully covered. Five-bilayer PAH/PSS membranes have Cl^-/SO_4^{2-} and $Cl^-/Fe(CN)_6^{3-}$ selectivity values of 7 and 310, respectively. PAH/poly(acrylic acid) membranes show selectivity values similar to those of PAH/PSS membranes but with a 3-fold decrease in anion flux. Selectivity in both of these systems likely results from Donnan exclusion.

Introduction

We report the synthesis of ultrathin, layered polyelectrolyte membranes on porous alumina substrates. Field-emission scanning electron microscope (FESEM) images show that as few as five bilayers (<25 nm) of polyelectrolyte effectively cover the surface without filling of underlying pores. These films form ultrathin barriers that allow high flux along with selective transport of anions, where anion charge and size determine selectivity.

Anion separation membranes have a long history including applications in salt production from seawater,[1−3] acid and dye recovery from brine solutions,[4−7] separation of organic acids during food processing,[8] sensors,[9,10] and separation of pollutants from groundwater.[11−13] The properties (e.g., hydrophilicity,[2,3,14−16] charge,[6,17] and degree of cross-linking[1,8]) of the polymer membrane dictate flux and selectivity. Although polymer membranes are used extensively, large membrane thicknesses often limit flux.[4,6,14,15,18,19] Ultrathin, layered polyelectrolyte films with deposition restricted to a support surface should overcome this limitation. Additionally, many different types of polyelectrolytes can form layered films, allowing for possible tailoring of membrane selectivity.

Ultrathin membranes are attractive for separation processes because they can simultaneously allow both high flux and high permselectivty.[20−22] Typically, ultrathin membranes are polymer "skins" (<50 nm thick) on a highly permeable support.[22] The support provides mechanical stability, but its high permeability presents minimal mass-transfer resistance. Martin and co-workers used ultrathin polymer membranes deposited on porous alumina substrates in the development of anion-permselective sensors as well as gas-separation membranes.[10,20−23] Regen showed that even Langmuir−Blodgett films offer permselectivity in some gas separations.[24−27] Deposition of highly selective, stable, ul-

* To whom correspondence should be addressed. Phone: (517) 355−9715 ext. 237. Fax: (517) 353-1793. E-mail: bruening@cem.msu.edu.

(1) Sata, T. *J. Membr. Sci.* **1994**, *93*, 117−135.
(2) Sata, T.; Yamaguchi, T.; Kawamura, K.; Matsusaki, K. *J. Chem. Soc., Faraday Trans.* **1997**, *93*, 457−462.
(3) Saracco, G.; Zanetti, M. C. *Ind. Eng. Chem. Res.* **1994**, *33*, 96−101.
(4) Moon, P. J.; Parulekar, S. J.; Tsai, S. *J. Membr. Sci.* **1998**, *141*, 75−89.
(5) Nam, S. Y.; Lee, Y. M. *J. Membr. Sci.* **1997**, *135*, 161−171.
(6) Stachera, D. M.; Childs, R. F.; Mika, A. M.; Dickson, J. M. *J. Membr. Sci.* **1998**, *148*, 199−127.
(7) Xu, X.; Spencer, G. *Desalination* **1997**, *114*, 129−137.
(8) Gudernatsch, W.; Krumbholz, C. H.; Strathmann, H. *Desalination* **1990**, *79*, 249−260.
(9) Toniolo, R.; Comisso, N.; Bontempelli, G.; Schiavon, G.; Sitran, S. *Electroanalysis* **1998**, *10*, 942−947.
(10) Ugo, P.; Moretto, L. M.; Mazzocchin, G. A.; Guerriero, P.; Martin, C. R. *Electroanalysis* **1998**, *10*, 1168−1173.
(11) Fryxell, G. E.; Liu, J.; Hauser, T. A.; Nie, Z.; Ferris, K. F.; Mattigod, S.; Gong, M.; Hallen, R. T. *Chem. Mater.* **1999**, *11*, 2148−2154.
(12) Hell, F.; Lahnsteiner, J.; Frischherz, H.; Baumgartner, G. *Desalination* **1998**, *117*, 173−180.
(13) Sata, T.; Yamaguchi, T.; Matsusaki, K. *J. Chem. Soc., Chem. Commun.* **1995**, 1153−1154.
(14) Sata, T.; Yamaguchi, T.; Matsusaki, K. *J. Phys. Chem.* **1995**, *99*, 12875−12882.
(15) Sata, T.; Mine, K.; Higa, M. *J. Membr. Sci.* **1998**, *141*, 137−144.
(16) Sata, T.; Tagami, Y.; Matsusaki, K. *J. Phys. Chem. B* **1998**, *102*, 8473−8479.
(17) Mika, A. M.; Childs, R. F.; Dickson, J. M.; McCarry, B. E.; Gagnon, D. R. *J. Membr. Sci.* **1997**, *135*, 81−92.
(18) Zeng, X.; Ruckenstein, E. *J. Membr. Sci.* **1998**, *148*, 195−205.
(19) Narebska, A.; Warszawski, A. *Sep. Sci. Technol.* **1992**, *27*, 703−715.
(20) Liu, C.; Espenscheid, M. W.; Chen, W.-J.; Martin, C. R. *J. Am. Chem. Soc.* **1990**, *112*, 2.
(21) Liang, W.; Martin, C. R. *Chem. Mater.* **1991**, *3*, 390−391.
(22) Liu, C.; Martin, C. R. *Nature* **1991**, *352*, 50−52.
(23) Liu, C.; Chen, W. J.; Martin, C. R. *J. Membr. Sci.* **1992**, *65*, 113−128.
(24) Dedek, P.; Webber, A. S.; Janout, V.; Hendel, R. A.; Regen, S. L. *Langmuir* **1994**, *10*, 3943−3945.

10.1021/cm0001004 CCC: $19.00
Published on Web 06/23/2000

trathin membranes remains a challenge, however, because of the difficulty of fully covering a porous substrate without filling of the pores.

Layer-by-layer deposition of polyelectrolytes offers an attractive means of depositing a variety of charged, ultrathin membranes.[28−30] Synthesis of layered polyelectrolyte films involves alternating immersions of a charged substrate into solutions of oppositely charged polyelectrolytes.[30] The layer-by-layer procedure provides control of film thickness on the nanometer scale. Initial research on these films focused on fundamental aspects such as controlling bilayer thickness,[31] layer interpenetration,[32−34] and bilayer composition,[35−40] while recent reports focus on the benefits of polyelectrolyte films in fields ranging from coatings to separations.[41,42] Several groups report the use of polyelectrolyte films to modify polymer substrates for gas separation.[43−46] These studies show that selectivity depends on the number of polyelectrolyte layers, substrate properties, and the polyelectrolytes used in film deposition.[43−46] A recent study showed that the multibipolar structure of polyelectrolyte films is useful in the separation of mono- and divalent ions.[42] The selective ion transport through these films appears to be due to Donnan exclusion of the divalent ion. However, in all reports of layered polyelectrolyte membranes,[42−46] little emphasis is placed on the formation of a true ultrathin membrane and whether film deposition occurs at the membrane surface or within the substrate pores. We report on the structure of polyelectrolyte films deposited on porous alumina substrates and the transport of mono-, di-, and trivalent anions of varying size through these ultrathin membranes.

Experimental Section

Materials. Poly(allylamine hydrochloride) (PAH) (Aldrich, M_w = 70 000), poly(styrenesulfonate) (PSS) (Aldrich, M_w = 70 000), poly(acrylic acid) (PAA) (M_w = 90,000, 25 wt % solution, Alfa Aesar), $MnCl_2$ (Mallinckrodt), NaBr (Aldrich), NaCl (Mallinckrodt), $K_2Ni(CN)_4$ (Aldrich), KCl (Baker), KNO_3 (CCI), K_2SO_4 (CCI), $K_3Fe(CN)_6$ (Mallinckrodt), and salicylic acid (Spectrum) were used as received. Prior to film deposition, the porous alumina support (Whatman Anodisc 0.02 μm membrane filters) was UV/O_3 cleaned for 15 min (Boekel UV_Clean model 135500). Polyelectrolyte deposition began by immersing the alumina support in a solution of PAH (0.02 M with respect to the monomer unit, pH = 2.3 for PAH/PSS films or pH = 4.5 for PAH/PAA films) for 5 min. PAH solutions also contained either 0.5 M NaBr (PAH/PSS deposition) or 0.5 M NaCl (PAH/PAA deposition). Supporting electrolytes were chosen on the basis of literature preparations of polyelectrolyte films.[31,47,48] The alumina membrane has two distinct sides: the filtrate side has a skin layer of 0.02 μm diameter pores and the permeate side has 0.2 μm diameter pores. We limited polyelectrolyte deposition to the filtrate side using a holder. A 1-min rinse with water (Milli-Q, 18 MΩ-cm) followed PAH deposition and all other polyelectrolyte deposition steps. To deposit the polyanion, the PAH-coated alumina support was immersed in either a solution of PSS (0.02 M with respect to the monomer unit, pH = 2.1, 0.5 M $MnCl_2$) for 2 min or a solution of PAA (0.02 M with respect to the monomer unit, pH = 4.5, 0.5 M NaCl) for 5 min. After the deposition of the desired number of polyelectrolyte layers, the membrane was dried with N_2. A Hitachi S-4700 FESEM (V_{ac} = 6−8 kV) was used to image polyelectrolyte films deposited on alumina membranes. The use of low voltages with the FESEM allows imaging of polymer films while reducing charging artifacts and specimen damage.[49,50] Samples were coated with 5 nm of Au for FESEM imaging.

Although we first exposed the substrate to the polycation, PAH, the Al_2O_3 support should be positively charged under the conditions of this study,[51] limiting polycation adsorption. Ellipsometric and Fourier transform infrared−external reflectance spectroscopy experiments show that little PAH adsorbs directly onto the native oxide of Al-coated Si wafers, but direct adsorption of PAA on Al is also difficult to detect. We compared transport properties of a nominal five-bilayer PAH/PSS membrane and a 4.5-bilayer PSS/PAH membrane. Anion fluxes through these two membranes are indistinguishable.

Transport Studies. The dialysis apparatus consists of two glass cells (volumes of 100 mL) connected by a 2.5-cm-long neck in which the membrane separates the feed and permeate sides. The exposed area of the membrane was 2.0 cm^2. The permeate cell contained Milli-Q water and the feed cell contained the appropriate 0.1 F salt solution (KCl, KNO_3, K_2SO_4, $K_2Ni(CN)_4$, and $K_3Fe(CN)_6$). The measured pH values of the unbuffered 0.1 F salt solutions were 4.8 (KCl), 5.3 (KNO_3), 5.5 (K_2SO_4), 6.4 ($K_2Ni(CN)_4$), and 6.2 ($K_3Fe(CN)_6$). These pH values are well below the pK value for ammonium groups and well above the pK value of styrene sulfonic acid. Thus, pH should have little effect on transport in this system. However, in the case of PAH/PAA membranes, there is a possibility that pH may affect transport. As the selectivities in the PAH/PAA system were similar to those of PAH/PSS, we assume that the pH differences in these unbuffered solutions have little effect on transport. Salicylic acid (SA) was also used as a probe anion. Solutions of salicylic acid were adjusted to a pH of 6 with KOH to deprotonate the acid. The concentration of salt in the permeate cell was monitored at 10 min intervals for 90 min

(25) Albrecht, O.; Laschewsky, A.; Ringsdorf, H. *Macromolecules* **1984**, *17*, 937−940.
(26) Hendel, R. A.; Nomura, E.; Janout, V.; Regen, S. L. *J. Am. Chem. Soc.* **1997**, *119*, 6909−6918.
(27) Conner, M. D.; Janout, V.; Kudelka, I.; Dedek, P.; Zhu, J.; Regen, S. L. *Langmuir* **1993**, *9*, 2389−2397.
(28) Decher, G.; Hong, J. D. *Ber. Bunsen-Ges. Phys. Chem.* **1991**, *95*, 1430−1434.
(29) Decher, G.; Hong, J.-D.; Schmitt, J. *Thin Solid Films* **1992**, *210*, 831−835.
(30) Decher, G. *Science* **1997**, *277*, 1232−1237.
(31) Yoo, D.; Shiratori, S. S.; Rubner, M. F. *Macromolecules* **1998**, *31*, 4309−4318.
(32) Baur, J. W.; Rubner, M. F.; Reynolds, J. R.; Kim, S. *Langmuir* **1999**, *15*, 6460−6469.
(33) Lösche, M.; Schmitt, J.; Decher, G.; Bouwman, W. G.; Kjaer, K. *Macromolecules* **1998**, *31*, 8893−8906.
(34) Schlenoff, J. B.; Ly, H.; Li, M. *J. Am. Chem. Soc.* **1998**, *120*, 7626−7634.
(35) Ariga, K.; Lvov, Y.; Kunitake, T. *J. Am. Chem. Soc.* **1997**, *119*, 2224−2231.
(36) Lvov, Y.; Decher, G.; Sukhorukov, G. *Macromolecules* **1993**, *26*, 5396−5399.
(37) Lvov, Y.; Haas, H.; Decher, G.; Möhwald, H. *Langmuir* **1994**, *10*, 4232−4236.
(38) Lvov, Y.; Ariga, K.; Ichinose, I.; Kunitake, T. *J. Am. Chem. Soc.* **1995**, *117*, 6117−6123.
(39) Lvov, Y. M.; Lu, Z.; Schenkman, J. B.; Zu, X.; Rusling, J. F. *J. Am. Chem. Soc.* **1998**, *120*, 4073−4080.
(40) Laschewsky, A.; Mayer, B.; Wischerhoff, E.; Arys, X.; Jones, A. *Ber. Bunsen-Ges. Phys. Chem.* **1996**, *100*, 1033−1038.
(41) Graul, T. W.; Schlenoff, J. B. *Anal. Chem.* **1999**, *71*, 4007−4013.
(42) Krasemann, L.; Tieke, B. *Langmuir* **2000**, *16*, 287−290.
(43) Ackern, F. v.; Krasemann, L.; Tieke, B. *Thin Solid Films* **1998**, *327−329*, 762−766.
(44) Kotov, N. A.; Magonov, S.; Tropsha, E. *Chem. Mater.* **1998**, *10*, 886−895.
(45) Stroeve, P.; Vasquez, V.; Coelho, M. A. N.; Rabolt, J. F. *Thin Solid Films* **1996**, *284−285*, 708−712.
(46) Leväsalmi, J.-M.; McCarthy, T. J. *Macromolecules* **1997**, *30*, 1752−1757.
(47) Caruso, F.; Niikura, K.; Furlong, D. N.; Okahata, Y. *Langmuir* **1997**, *13*, 3422−3426.
(48) Decher, G.; Lvov, Y.; Schmitt, J. *Thin Solid Films* **1994**, *244*, 772−777.
(49) Kim, K. Y.; Dickson, M. R.; Chen, V.; Fane, A. G. *Micron Microscopia Acta* **1992**, *23*, 259−271.
(50) Kim, K. J.; Fane, A. G. *J. Membr. Sci.* **1994**, *88*, 103−114.
(51) Parks, G. A. *Chem. Rev.* **1965**, *65*, 177−198.

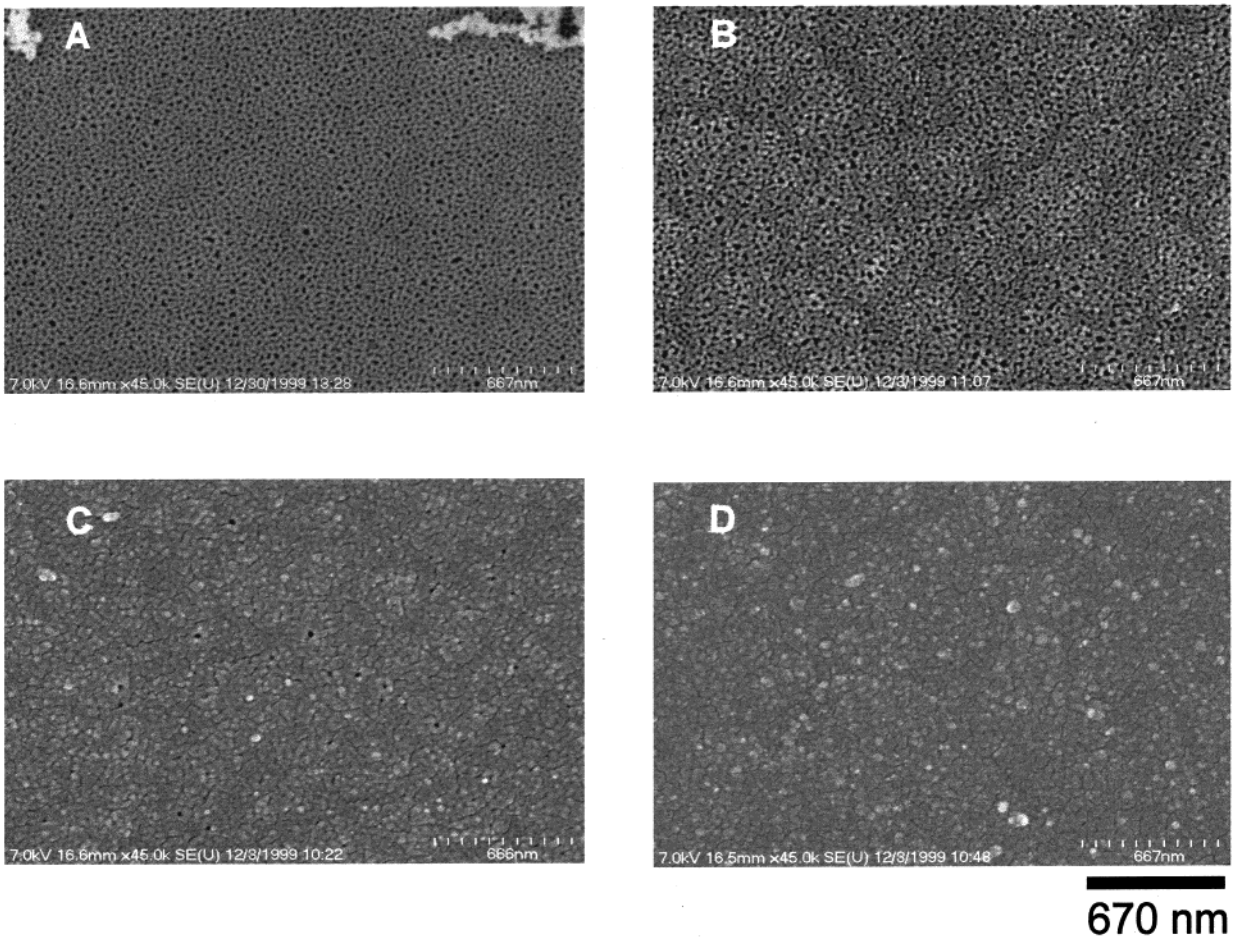

Figure 1. FESEM images of the filtrate side of porous alumina substrates before (A) and after coating with two (B), four (C), or five (D) PAH/PSS bilayers.

using conductivity measurements (Orion model 115 conductivity meter). To normalize receiving phase conductivity values, we divide by the conductivity of the source phase. Both feed and permeate solutions were stirred vigorously to minimize concentration polarization at the membrane surface. Permeability measurements made with different stirring speeds showed no significant change in flux. The order in which the anions were investigated was Cl^-, NO_3^-, SO_4^{2-}, $Ni(CN)_4^{2-}$, and $Fe(CN)_6^{3-}$. After determining the flux of each anion, the membrane was immersed in Milli-Q water for 15 min.

The integrity of the film during the permeability experiments was tested with a second Cl^- run performed after the experiment with $Fe(CN)_6^{3-}$. The Cl^- flux changed less than 10% for PAH/PSS membranes, but PAH/PAA membranes showed a ~50% decrease. Three or more different membranes were tested for each type of polyelectrolyte film.

Results and Discussion

To synthesize ultrathin polyelectrolyte membranes, the layered film must cover the substrate without filling underlying pores. Although a few reports describe the layer-by-layer deposition of polyelectrolyte films on highly porous substrates,[5,43−46] they do not emphasize surface coverage or the likely possibility of polyelectrolyte deposition in substrate pores. FESEM images (Figure 1) of PAH/PSS films on porous alumina show that coverage of the filtrate side of the membrane gradually increases with the deposition of each subsequent bilayer. Complete pore coverage occurs after the addition of about five PAH/PSS bilayers. Micrographs of the alumina permeate side (Figure 2) show that this surface remains polyelectrolyte free even after deposition of ten bilayers on the filtrate side. This demon-

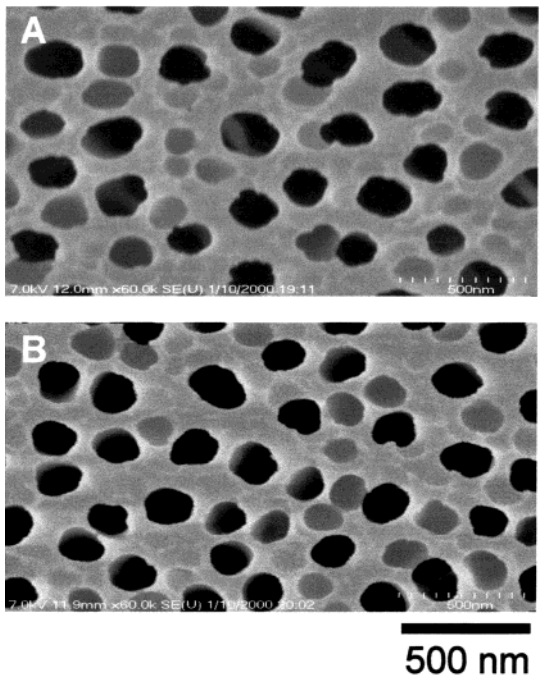

Figure 2. FESEM images of the permeate side of a bare porous alumina substrate before (A) and after (B) deposition of ten PAH/PSS bilayers on the filtrate side of the alumina support.

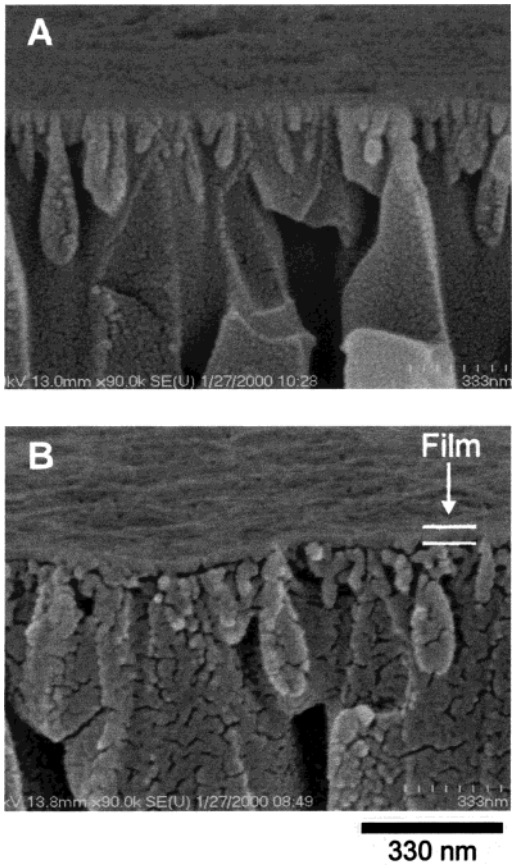

Figure 3. Cross-sectional FESEM image of porous alumina substrates before (A) and after (B) coating with ten PAH/PSS bilayers. Film thickness is about 40 nm.

strates that deposition of the polyelectrolyte does not occur throughout the membrane. FESEM micrographs of five-bilayer PAH/PAA membranes also show a defect free film, but complete pore coverage occurs with fewer depositions as the bilayer thickness of PAH/PAA films is greater than that of PAH/PSS films.

Cross-sectional FESEM images show that the pores of the membrane are unblocked after film deposition. Figure 3 shows a ten-bilayer PAH/PSS film deposited on the membrane surface (filtrate side), with little polyelectrolyte in the alumina pores. There appears to be some polyelectrolyte in the upper part of the pores as the appearance of small cracks is likely due to a small amount of polyelectrolyte deposition. However, the majority of film deposition occurs at the support surface and the pores remain open, even if they contain a bilayer or two of polyelectrolyte. Figure 4 shows the interior pore structure of an alumina support that was coated with a ten-bilayer PAH/PSS film. The absence of polyelectrolyte in this image shows that polyelectrolytes are unable to penetrate much past the skin layer on the filtrate side of the support. The cross-sectional micrograph of the ten-bilayer PAH/PSS membrane (Figure 3) indicates a film thickness of ~40 nm, which is comparable to ellipsometric thicknesses for ten-bilayer films deposited on solid substrates.[52] Images in Figures 1−4 show collectively that deposition of layered polyelectrolyte films is a simple means of creating ultrathin membranes on porous supports.

(52) Harris, J. J.; Bruening, M. L. *Langmuir* **2000**, *16*, 2006−2013.

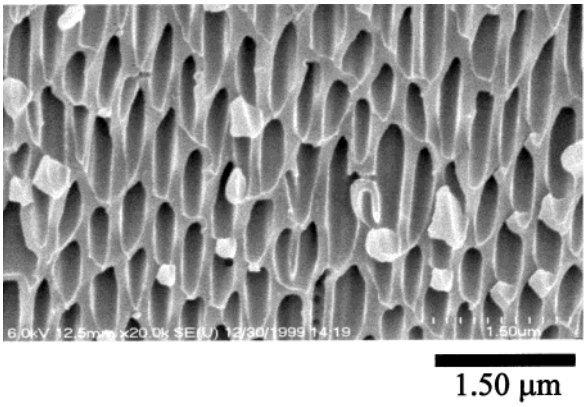

Figure 4. FESEM image showing the interior of a porous alumina support that had ten PAH/PSS bilayers deposited on the filtrate side.

Because pore coverage depends on the number of polyelectrolyte bilayers, selectivity and flux through these membranes also vary with the number of PAH/PSS bilayers. Chloride flux shows little change with the number of PAH/PSS bilayers, while SO_4^{2-} transport decreases 5-fold with the addition of ten bilayers (Table 1). Under the same conditions, $Fe(CN)_6^{3-}$ flux decreases 330-fold. Figure 5, which shows receiving phase conductivity as a function of time, illustrates the effect of each additional PAH/PSS bilayer on SO_4^{2-} flux. The selectivity ratio for Cl^- to SO_4^{2-}, which is determined by dividing anion flux values, reaches its maximum value of 7 after the deposition of five bilayers.[53] This is consistent with the FESEM images that show complete surface coverage with few defects after the deposition of five bilayers (Figure 1). Prior to complete pore coverage, most sulfate transport likely occurs through membrane defects. Upon full coverage, however, sulfate must enter and diffuse through the membrane causing a decrease in flux. Resistance to mass transfer of Cl^- through the polyelectrolyte film must be minimal because flux is hardly affected by full coverage of the support.

Figure 6 compares the fluxes of various anions through a five-bilayer PAH/PSS membrane. The smallest measured fluxes for PAH/PSS membranes occur with $Fe(CN)_6^{3-}$, because its high charge produces the largest electrostatic repulsion between anion and membrane. The linearity of the conductivity values with time, which occurs with each membrane tested, demonstrates steady-state anion transport where receiving-phase concentration is negligible compared to that in the source phase. Five-bilayer PAH/PSS membranes show selectivity ratios of 300, 50, and 20 for $Cl^-/Fe(CN)_6^{3-}$, $SO_4^{2-}/Fe(CN)_6^{3-}$, and $Ni(CN)_4^{2-}/Fe(CN)_6^{3-}$, respectively (Table 1 and Figure 6). The ability of PAH/PSS membranes to nearly eliminate $Fe(CN)_6^{3-}$ flux suggests that these membranes could be useful for the dialytic purification of large, highly charged molecules.[18,54−56]

(53) Selectivity values can be calculated directly from flux ratios because source-phase concentrations were always 0.1 F.

(54) Åkerman, S.; Viinikka, P.; Svarfvar, B.; Järvinen, K.; Kontturi, K.; Näsman, J.; Urtti, A.; Paronen, P. *J. Controlled Release* **1998**, *50*, 153−166.

(55) Chen, D.-H.; Wang, S.-S.; Huang, T.-C. *J. Chem. Technol. Biotechnol.* **1995**, *64*, 284−292.

Table 1. Anion Fluxes (mol cm^{-2} s^{-1}) through Porous Alumina Supports Coated with Polyelectrolyte Membranes of Varying Layer Number and Composition[a]

number of bilayers	Cl^- flux	NO_3^- flux	SO_4^{2-} flux	$Ni(CN)_4^{2-}$ flux	$Fe(CN)_6^{3-}$ flux
0	$6.7 \times 10^{-8} \pm 3\%$	$6.5 \times 10^{-8} \pm 10\%$	$4.9 \times 10^{-8} \pm 5\%$	$4.9 \times 10^{-8} \pm 2\%$	$4.6 \times 10^{-8} \pm 5\%$
1 PAH/PSS	$6.6 \times 10^{-8} \pm 4\%$		$4.8 \times 10^{-8} \pm 6\%$		$4.4 \times 10^{-8} \pm 10\%$
2 PAH/PSS	$5.7 \times 10^{-8} \pm 7\%$		$4.5 \times 10^{-8} \pm 3\%$		$4.1 \times 10^{-8} \pm 7\%$
3 PAH/PSS	$5.9 \times 10^{-8} \pm 5\%$		$2.9 \times 10^{-8} \pm 8\%$		$1.3 \times 10^{-8} \pm 40\%$
4 PAH/PSS	$5.1 \times 10^{-8} \pm 13\%$		$1.5 \times 10^{-8} \pm 14\%$		$2.7 \times 10^{-9} \pm 10\%$
5 PAH/PSS	$6.5 \times 10^{-8} \pm 25\%$	$6.1 \times 10^{-8} \pm 20\%$	$9.9 \times 10^{-9} \pm 8\%$	$4.7 \times 10^{-9} \pm 10\%$	$2.1 \times 10^{-10} \pm 30\%$
5.5 PAH/PSS	$4.6 \times 10^{-8} \pm 6\%$	$5.0 \times 10^{-8} \pm 4\%$	$2.2 \times 10^{-8} \pm 20\%$	$8.6 \times 10^{-9} \pm 30\%$	$1.9 \times 10^{-10} \pm 20\%$
10 PAH/PSS	$4.5 \times 10^{-8} \pm 1\%$	$5.1 \times 10^{-8} \pm 4\%$	$8.9 \times 10^{-9} \pm 1\%$	$3.6 \times 10^{-9} \pm 3\%$	$1.4 \times 10^{-10} \pm 20\%$
5 PAH/PAA	$1.6 \times 10^{-8} \pm 10\%$	$1.7 \times 10^{-8} \pm 6\%$	$3.7 \times 10^{-9} \pm 30\%$	$3.6 \times 10^{-10} \pm 11\%$	$7.1 \times 10^{-11} \pm 20\%$

[a] Initially the source compartment contained a 0.1 F solution of the appropriate salt and the receiving compartment contained deionized water. Flux values were calculated from the receiving phase concentration after 90 min. The standard deviations are from measurements with three or more different membranes.

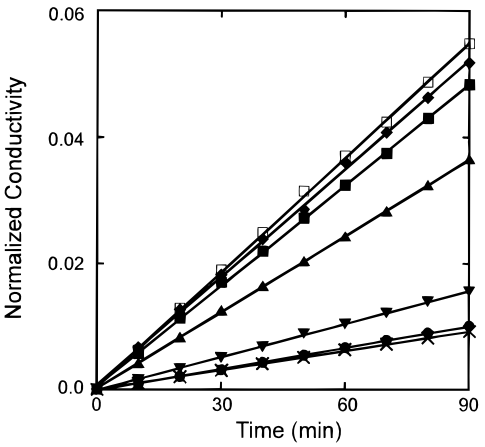

Figure 5. Plot of normalized receiving phase conductivity as a function of time when the source phase contained 0.1 F K_2SO_4. Representative data are shown for a bare porous alumina support (open squares) and for alumina coated with one (diamonds), two (squares), three (triangles), four (inverted triangles), five (circles), or ten bilayers (X's) of PAH/PSS.

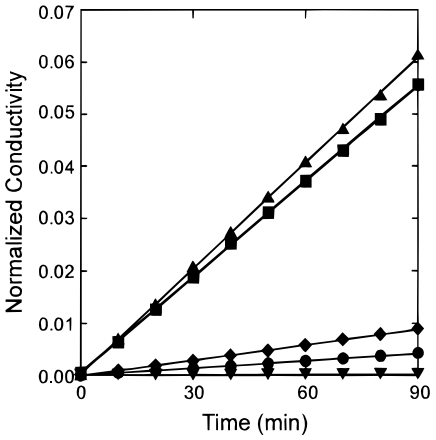

Figure 6. Normalized receiving phase conductivity as a function of time when the source phase (0.1 F salt) is separated from the receiving phase by a five-bilayer PAH/PSS membrane: KCl (triangles), KNO_3 (squares), K_2SO_4 (diamonds), $K_2Ni(CN)_4$ (circles), and $K_3Fe(CN)_6$ (inverted triangles).

Once complete pore coverage occurs, the presence of additional polyelectrolyte bilayers decreases anion flux, but has little impact on selectivity.[57] The Cl^-/SO_4^{2-}, $Cl^-/Fe(CN)_6^{3-}$, $Cl^-/Ni(CN)_4^{2-}$, and $SO_4^{2-}/Ni(CN)_4^{2-}$ selectivity are nearly the same for five- and ten-bilayer PAH/PSS membranes. On going from five to ten PAH/PSS bilayers, anion flux decreases only between 10 and 30% (Table 1).

The minimal decrease in flux of highly charged anions on going from five- to ten-bilayer membranes suggests that the major selectivity factor is Donnan exclusion near the surface.[42] Hindered diffusion would yield a significant decrease in anion flux with increasing membrane thickness, while Donnan exclusion due to uncompensated charge at the membrane surface should be relatively constant once full coverage is achieved.[42,58] The large decreases in SO_4^{2-}, $Ni(CN)_4^{2-}$, and $Fe(CN)_6^{3-}$ fluxes upon addition of the first five PAH/PSS bilayers likely result from increased Donnan exclusion as surface coverage increases. Also consistent with a Donnan exclusion model is the much smaller reduction in Cl^- and NO_3^- flux (Table 1) due to the much smaller repulsive forces generated by the monovalent anions. One advantage of an electrostatic exclusion mechanism in PAH/PSS membranes is that it provides monovalent/divalent and monovalent/trivalent selectivity with little inhibition of the monovalent anion flux (Table 1).

The majority of uncompensated charge lies near the film/solution interface[34,59] so one should expect a change in anion flux if the outer layer is a polycation rather than a polyanion. We tested this possibility by depositing an additional PAH layer on a five-bilayer film. This yields a membrane with a positive surface charge, while providing a minimal change in membrane thickness. The additional PAH layer has little effect on Cl^- and NO^{3-} transport (Table 1) as the flux of these anions is already close to that of bare alumina. However, there is a 2-fold increase in SO_4^{2-} and $Ni(CN)_4^{2-}$ flux when the outermost charge is positive (Table 1). This suggests that the outer-layer charge does have a significant effect on flux. In contrast, there is little change in $Fe(CN)_6^{3-}$ flux when the outer-layer charge is positive. Apparently, large repulsive forces between internal regions of the membrane and trivalent $Fe(CN)_6^{3-}$ are dominant for decreasing $Fe(CN)_6^{3-}$ flux. This is somewhat surprising as Schlenoff showed that strongly dissociated polyelectrolytes provide complete intrinsic charge compensation.[34] However, charge compensation appears to depend on deposition conditions and the polyelectrolyte used.[60] For PAH/PSS films Lowack and

(56) Saimoto, H.; Shigemasa, Y. *Polym. Adv. Technol.* **1999**, *10*, 39−42.

(57) A recent report by Krasemann and Tieke shows that transport selectivity does depend on the number of PAH/PSS bilayers. However, these films are deposited under different conditions and on different supports.

(58) Lowack, K.; Helm, C. A. *Macromolecules* **1998**, *31*, 823−833.

(59) Dubas, S. T.; Schlenoff, J. B. *Macromolecules* **1999**, *32*, 8153−8160.

Helm suggest significant extrinsic charge compensation which could result in Donnan exclusion within the polyelectrolyte membrane.[58]

Flux of the potassium salt of salicylic acid through PAH/PSS films supports the hypothesis that Donnan exclusion (rather than hindered diffusion) is the dominant factor governing transport selectivity. We chose to work with salicylate because it is a large monovalent anion with a diffusion coefficient 15% smaller than that of $Fe(CN)_6^{3-}$.[61] The large size of salicylate is manifested by the fact that its flux through bare alumina (3.2×10^{-8} mol cm^{-2} s^{-1}) is the lowest of any anion tested. The presence of five PAH/PSS bilayers on alumina reduces salicylate flux 2-fold while reducing Cl^- flux by <30%. This suggests some size selectivity between monovalent anions. However, most selectivity among anions occurs as a result of Donnan exclusion as shown by the fact that five PAH/PSS bilayers reduce $Fe(CN)_6^{3-}$ flux 220-fold and SO_4^{2-} flux 5-fold. This occurs although salicylate, SO_4^{2-}, and $Fe(CN)_6^{3-}$ have similar diffusion coefficients.[61,62] These results show that Donnan exclusion is the major factor affecting anion transport, but there may be some effect of size for larger anions.

Transport selectivity is similar in PAH/PAA and PAH/PSS membranes, although fluxes are considerably lower through PAH/PAA membranes. Five-bilayer PAH/PAA membranes show between a 2- and 10-fold reduction in anion flux compared to ten-bilayer PAH/PSS membranes (Table 1), which have similar thicknesses as seen with FESEM. The Cl^-/SO_4^{2-} and $Cl^-/Fe(CN)_6^{3-}$ selectivity values for PAH/PAA films, 4 and 230, respectively, are similar to ten-bilayer PAH/PSS selectivity values. The decreases in anion flux are likely due to a tighter structure in PAH/PAA membranes than in PAH/PSS membranes. If the effect was due to higher charge densities, we would expect to see higher Cl^-/SO_4^{2-} selectivities but this is not the case.

Decreased flux through PAH/PAA membranes is in contrast to our previous work with PAH/PAA films deposited on gold electrodes.[52] In those studies, cyclic voltammetry of $Fe(CN)_6^{3-}$ was hardly affected by the presence of five bilayers of PAH/PAA, suggesting rapid $Fe(CN)_6^{3-}$ flux through these films. We speculate that in the present case, PAH/PAA swelling is constricted at the surface of the alumina pores. Swelling of films on solid gold electrodes is uninhibited and may result in an open and highly permeable film.

Ultrathin polyelectrolyte films on porous supports show selectivities typical of anion exchange membranes. Using five-bilayer PAH/PSS membranes on Celgard supports, Krasemann and Tieke report a Cl^-/SO_4^{2-} selectivity value of 17, which is somewhat higher than our value of 7.[42] This higher value may be a result of a different film structure due to a difference in preparation conditions or substrate topography. Our Cl^-/SO_4^{2-} selectivity value of 7 is 2-fold higher than a previous dialysis study using interpolymer type carboxylic ion-exchange membranes.[63] Electrodialysis studies with copolymer membranes show selectivity values between 1 and 100, where higher values usually result from cross-linked surfaces.[1,2,14−16] Our ultrathin, polyelectrolyte membranes show average selectivity values, although they are significantly thinner than typical membranes. We are currently working on cross-linking polyelectrolyte membranes to increase their selectivity.

Acknowledgment. We acknowledge partial financial support from the Division of Chemical Sciences, Office of Energy Research, U.S. Department of Energy, Michigan State University, and the National Science Foundation (CHE-9816108).

CM0001004

(60) Hoogeveen, N. G.; Stuart, M. A. C.; Fleer, G. J.; Böhmer, M. R. *Langmuir* **1996**, *12*, 3675−3681.

(61) Stojek, Z.; Ciszkowska, M.; Osteryoung, J. G. *Anal. Chem.* **1994**, *66*, 1507−1512.

(62) Bard, A. J.; Faulkner, L. R. *Electrochemical Methods*; John Wiley & Sons: New York, 1980.

(63) Wycisk, R.; Trochimczuk, W. M. *J. Membr. Sci.* **1992**, *65*, 141−146.